nature neuroscience

Visualizing an emotional valence map in the limbic forebrain by TAI-FISH

Jianbo Xiu[1–3], Qi Zhang[1–3], Tao Zhou[1,2], Ting-ting Zhou[1,2], Yang Chen[1] & Hailan Hu[1]

A fundamental problem in neuroscience is how emotional valences are represented in the brain. We know little about how appetitive and aversive systems interact and the extent to which information regarding these two opposite values segregate and converge. Here we used a new method, tyramide-amplified immunohistochemistry–fluorescence *in situ* hybridization, to simultaneously visualize the neural correlates of two stimuli of contrasting emotional valence across the limbic forebrain at single-cell resolution. We discovered characteristic patterns of interaction, segregated, convergent and intermingled, between the appetitive and aversive neural ensembles in mice. In nucleus accumbens, we identified a mosaic activation pattern by positive and negative emotional cues, and unraveled previously unappreciated functional heterogeneity in the D1- and D2-type medium-spiny neurons, which correspond to the Go and NoGo pathways. These results provide insights into the coding of emotional valence in the brain and act as a proof of principle of a powerful methodology for simultaneous functional mapping of two distinct behaviors.

Emotions color our lives and drive behaviors[1,2]. Most emotions can be categorized along two dimensions: valence (value), ranging from negative to positive, and salience (arousal, intensity), ranging from weak to strong[3]. Although great advances have been made toward understanding the sensory representations of the external world[4–6], the manner in which different emotional valences are represented in the brain has remained largely elusive[7,8]. The major challenge is that many of the same brain regions are activated regardless of the stimulus being appetitive or aversive[9]. Unfortunately, functional magnetic resonance imaging, positron emission tomography or single-stimulus immediate early gene (IEG) mapping cannot resolve whether the activation occurs in the same or different neural populations in many commonly activated regions[9,10]. Pioneering electrophysiology studies have identified interesting patterns of neural activation to appetitive and aversive cues at various brain loci[11–16]; however, these studies sampled hundreds of neurons in one brain structure at a time, and the spatial relationship of the two neural ensembles in the entire structure and whole brain remains unclear.

To extract the valence representation of an emotion in the whole brain, we devised a strategy to compare the activity patterns evoked by two salient emotional stimuli with contrasting valence (morphine and foot shock) in the same mouse brain by improving a double-labeling technique based on the distinct induction time course of the mRNA and protein signals of the IEG gene *c-fos* (*Fos*)[17]. *c-fos* expression is generally low throughout the limbic nervous system in resting animals[18]; however, following neuronal activation, *c-fos* mRNA accumulates in minutes and decays in a couple hours, whereas its protein product appears slower and lasts much longer[19,20]. Thus, when two stimuli are sequentially applied at an appropriate interval, neural circuits activated by the two stimuli can be represented by the c-fos protein and mRNA signals, which in turn can be revealed by dual labeling using fluorescence immunohistochemistry (FIHC) and fluorescence *in situ* hybridization (FISH)[21] (**Fig. 1a**,**b**). For this dual-labeling approach to succeed, the *c-fos* mRNA and protein signals must be temporally separable: by the time the mRNA of the first stimulus decays, its protein signal should still be reasonably high (**Fig. 1a**). However, this criterion was not satisfied in many brain regions using regular immunohistochemistry and FISH (I-FISH, for example, in NAc; **Fig. 1c**). To overcome this problem, we used a tyramide-based step to amplify the immunohistochemical signal, resulting in a much better temporal separation of the mRNA and protein time courses and enabling mapping in many more brain regions (**Fig. 1c**). We named this technique tyramide-amplified IHC–FISH (TAI-FISH).

Using TAI-FISH dual labeling, we examined the *c-fos* activation patterns elicited by morphine and foot shock in the same mouse brain. We found that morphine and foot shock evoked largely distinct neural ensembles throughout the limbic forebrain, despite activating many of the same regions. As morphine and foot shock have different sensory properties, we also introduced additional pairs of emotional stimuli, including chocolate and restraint stress. In the nucleus accumbens (NAc), rewarding and aversive stimulus pairs (morphine/foot shock, morphine/restraint) recruited spatially intermingled neurons, whereas stimulus pairs of similar valence (morphine/chocolate, foot shock/restraint) activated largely overlapping neural groups, suggesting the existence of a functional valence map. This map partially, but not completely, coincides with the mosaic distribution of the Go and NoGo neurons defined by the D1 and D2 markers[22–24]. Our results provide insights into the internal representation of emotional valences and the functional organization of NAc. In addition, with the new amplification step allowing better separation of IEG mRNA and protein signals, TAI-FISH provides a much-needed molecular imaging technique for mapping the neural representations of two distinct behaviors across the whole brain at single-cell resolution.

[1]Institute of Neuroscience and State Key Laboratory of Neuroscience, Shanghai Institutes for Biological Sciences, Chinese Academy of Sciences, Shanghai, P.R. China. [2]Graduate School of Chinese Academy of Sciences, University of Chinese Academy of sciences, Shanghai, P.R. China. [3]These authors contributed equally to this work. Correspondence should be addressed to H.H. (hailan@ion.ac.cn).

Received 18 February; accepted 19 August; published online 21 September 2014; doi:10.1038/nn.3813

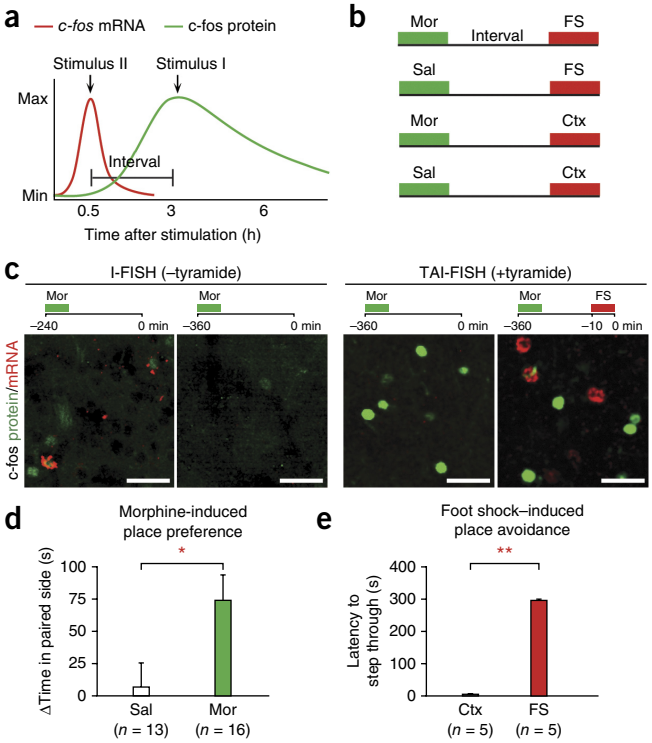

Figure 1 Use of TAI-FISH dual activity mapping to reveal the neural ensembles of appetitive and aversive emotional stimuli. (**a**) Schematic of the principle of dual activity mapping based on differential time courses of *c-fos* mRNA and protein expression. (**b**) Schematic of the experimental procedures, showing one dual labeling experiment, with morphine being the first stimulus and foot shock being the second, together with three parallel control experiments. Ctx, context; FS, foot shock; Mor, morphine; Sal, saline. (**c**) Importance of tyramide amplification of IHC signals. Note that, in I-FISH, without tyramide amplification, the IHC signal of the first stimulus was either mixed with the FISH signal at 240 min (left) or too weak by 360 min (middle left). With tyramide amplification, the IHC, but not the FISH, signal was observed for the first stimulus at 360 min (middle right), enabling the separate representation of the two stimuli (right). Images were taken in the NAc. Scale bars represent 30 µm. (**d**) Rewarding effect of morphine (single injection, 15 mg per kg, i.p.), as indicated by significantly increased time spent in the morphine-injected chamber in the conditioned place preference assay (Mann-Whitney *U* test, $*P < 0.05$). (**e**) Aversive effect of foot shock, as indicated by prolonged latency to step into shock chamber in conditioned place avoidance assay (Mann-Whitney *U* test, $**P < 0.01$). Error bars represent s.e.m.

RESULTS

Dual activity mapping of morphine and foot shock

To study the neural correlates of emotional valence, we applied TAI-FISH to visualize neural responses to morphine and foot shock, two emotional stimuli of contrasting valence. When morphine and foot shock were sequentially applied with an appropriate temporal interval, their neural correlates could be represented by the c-fos protein and mRNA signals, respectively (**Fig. 1a–c**). To elicit an appetitive response, we injected mice with morphine (15 mg per kg of body weight). At this dosage, a single intraperitoneal (i.p.) injection of morphine induced a preference for the injection chamber in the conditioned place preference test (**Fig. 1d**), confirming its appetitive nature[25]. For aversive stimulus, we applied foot shocks, which induced robust avoidance behavior in the passive avoidance test (**Fig. 1e**).

We first mapped the time courses for the *c-fos* mRNA and protein signals induced by morphine or foot shock alone. Mice were given either a single morphine injection or multiple electrical shocks, followed by 0, 20, 90, 180 or 360 min of rest in their home cage before being killed. In unstimulated mice, *c-fos* signals were uniformly low throughout the limbic forebrain, except in the paraventricular thalamus and suprachiasmatic nucleus, consistent with previous research[18]. Given the variation in the temporal profile of induced *c-fos* signals across different brain regions, we determined the optimal time intervals for each region for both stimuli to ensure that, at the time of

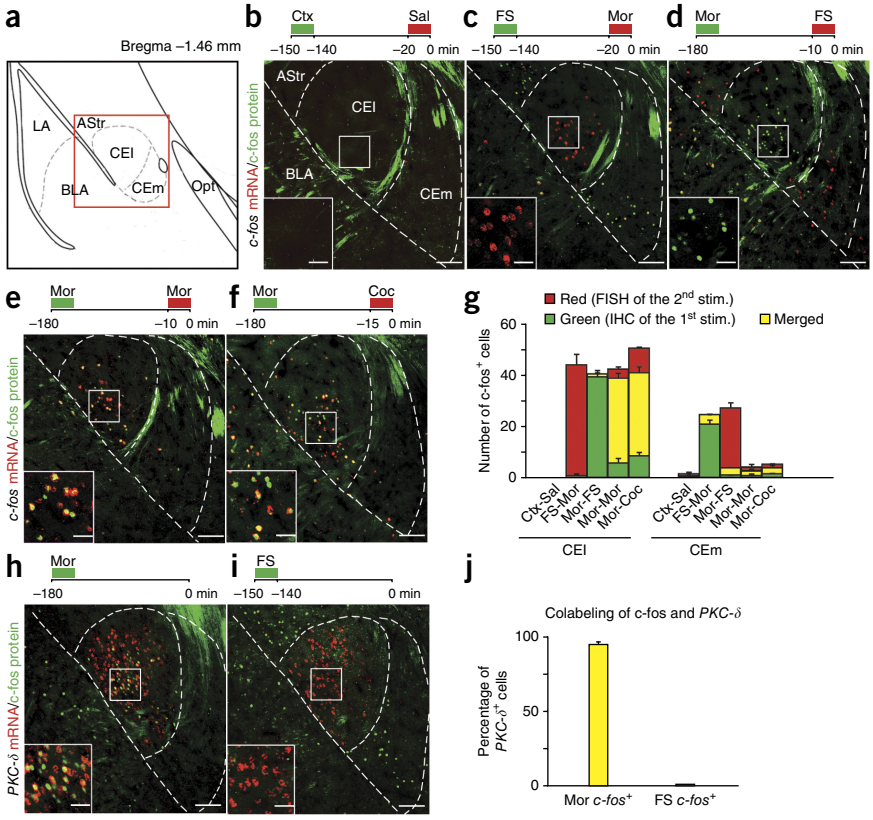

Figure 2 Segregated neural representations of morphine and foot shock in CEA. (**a**) Schematic illustrating the location of CEA. Red box indicates the position of the images shown in **b**–**i**. BLA, basal lateral amygdala; LA, lateral amygdala; opt, optic tract. (**b**–**f**) Representative images showing double labeling for c-fos protein (green) and mRNA (red) in CEA following sequential stimulation of context-saline (**b**), foot shock–morphine (**c**), morphine–foot shock (**d**), morphine-morphine (**e**) and morphine-cocaine (**f**). The green non-nuclear signals were a result of background staining caused by dense fibers in CEA, and were easily distinguishable from the cellular staining. (**g**) Statistics of red (expressing *c-fos* mRNA), green (expressing c-fos protein) and yellow (expressing both) neurons counted from the section shown in **e** and **f**. (**h**,**i**) Double staining for c-fos protein (green) and *PKC-δ* mRNA (red) following single stimulation of morphine (**h**) and foot shock (**i**). (**j**) Percentage of c-fos$^+$ neurons that also expressed *PKC-δ*, following single stimulation of morphine or foot shock. Scale bars represent 100 µm and 30 µm (insets). Error bars represent s.e.m.

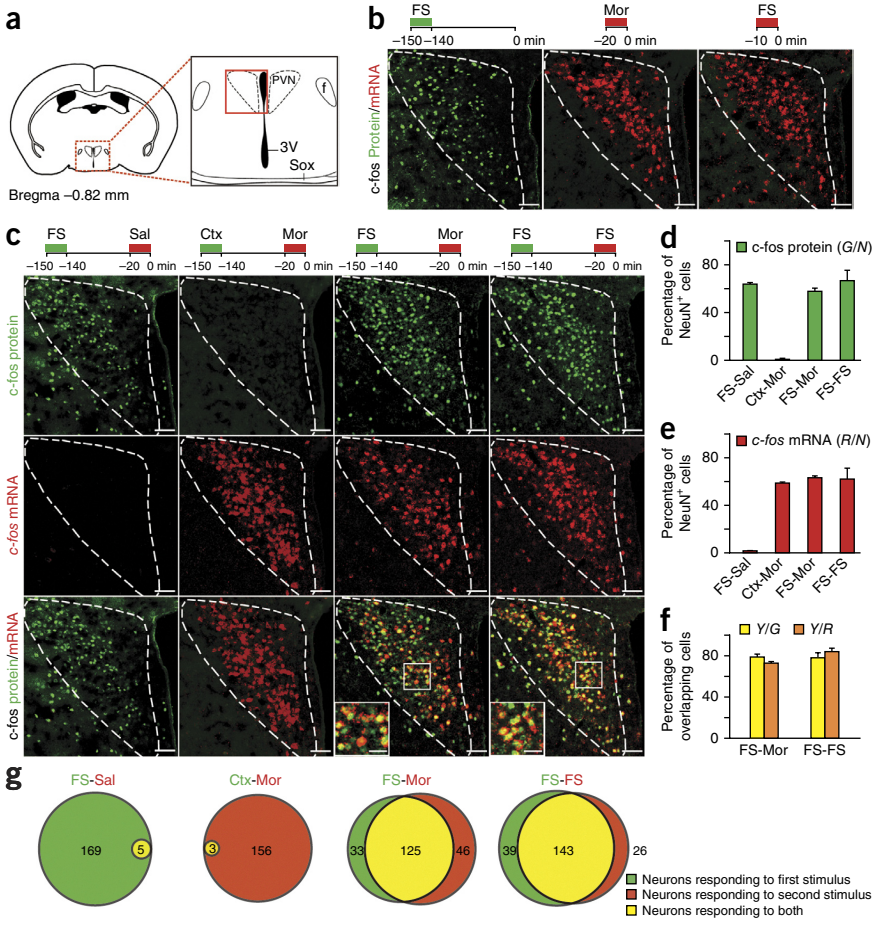

Figure 3 Convergent neural representations of morphine and foot shock in PVN. (**a**) Schematic illustrating the location of PVN. The red dashed box indicates the field of the image taken with a 10× objective. The red solid box indicates the position of the magnified images shown in **c**. 3V, third ventricle; f, fornix; sox, supraoptic decussation. (**b**) Only c-fos protein signals (green) were present at 150 min post foot shock and only *c-fos* mRNA signals (red) were present at 20 min post morphine and 10 min post foot shock. (**c**) Representative images showing green (c-fos protein), red (*c-fos* mRNA) and merged channels of I-FISH double labeling from four experiments: foot shock–saline, context-morphine, foot shock–morphine and foot shock–foot shock. (**d**,**e**) Percentage of neurons expressing c-fos protein (**d**) and mRNA (**e**) in PVN in the four experimental conditions. G, number of green neurons; R, number of red neurons; N, number of NeuN$^+$ neurons. (**f**) Percentage of overlap in the foot shock–morphine and foot shock–foot shock double-labeling experiments, as calculated by *Y/G* (yellow bar) or *Y/R* (orange bar). Y, number of yellow neurons. (**g**) Scaled Venn diagrams showing the number of green, red and yellow neurons in PVN in the four experimental conditions shown in **c**. Scale bars represent 50 µm and 20 µm (insets). Error bars represent s.e.m.

death, the *c-fos* mRNA induced by the first stimulus had decayed, whereas the c-fos protein induced by the second stimulus had not yet emerged (**Supplementary Figs. 1**–**3**). For double labeling, we then used FISH (in red) and FIHC (in green) to examine the mRNA and protein signals in the same brain slices.

We surveyed the whole limbic forebrain, particularly regions previously implicated in the response of morphine or foot shock, including NAc, lateral septum (LS), bed nucleus of the stria terminalis (BST), paraventricular nucleus of hypothalamus (PVN), central amygdala (CEA) and medial amygdala (MEA). In CEA, MEA and PVN, mRNA and protein signals were well-segregated, so we applied standard I-FISH without tyramide amplification of the IHC signal. In NAc, LS and BST, TAI-FISH was required and employed to assure good separation of the mRNA and protein signal time courses. We readily observed three spatial patterns of interaction between the neural ensembles for morphine and foot shock in the above limbic regions: segregated (where the two ensembles were spatially separated), convergent (where the two stimuli activated the same neurons) and intermingled (where they activated different neurons in the same region and signals were spatially mixed).

Segregated pattern in CEA, MEA, AStr and BSTov

In CEA, the nucleus essential for fear conditioning and expression[26,27] (**Fig. 2a**), exposure to the context of foot shock or saline injection in the home cage induced few signals (**Fig. 2b**). We then delivered foot shock and morphine injection 150 and 20 min before killing the mice, respectively, based on the time course of *c-fos* induction in this region (**Supplementary Figs. 1a** and **3a**). Notably, most foot shock–evoked green FIHC signals appeared in the medial division of CEA (CEm), whereas most morphine-activated red FISH signals were located in the lateral division (CEl), forming a clearly segregated pattern (**Fig. 2c**). We then reversed the temporal order of the stimuli, injecting morphine first and delivering foot shock second (morphine–foot shock configuration). The segregated pattern remained the same except that the colors were switched (**Fig. 2d**), suggesting that the temporal sequence of the two stimuli did not affect the pattern of signal distributions.

To further verify the technique, we injected the same (morphine; **Fig. 2e**) or a similar (cocaine; **Fig. 2f**) drug as the second stimulus after morphine injection. In both the morphine-morphine and morphine-cocaine configurations, red and green signals largely overlapped in the CEl region, with a 91 ± 3% overlap for morphine-morphine and 77 ± 2% overlap for morphine-cocaine double-stimulation (overlap ratio was calculated as the number of yellow neurons (*Y*) divided by the number of red neurons (*R*); note that *R* includes neurons that appeared either red or yellow; Online Methods and **Fig. 2e**–**g**). These observations suggest that, in general, the same neural populations in the CEl were repeatedly activated by the same or similar rewarding drugs.

Morphine and cocaine act via different routes to increase dopamine release; morphine binds to opiate receptors and inhibits the GABAergic neurons in the ventral tegmental area (VTA), whereas cocaine blocks dopamine reuptake at the synaptic sites[28]. Although opiate receptors are expressed in CEA, the great similarity that we observed in the activation pattern between the two drugs suggests that the neural activation, at least in the overlapping part, was most likely caused by increased dopamine release, rather than local opiate receptor activation outside VTA.

Elegant genetic and functional dissection of the CEA microcircuit has unraveled a subpopulation of neurons in the CEl region, CEl_{off}, which inhibits output neurons in the CEm and is essential for fear

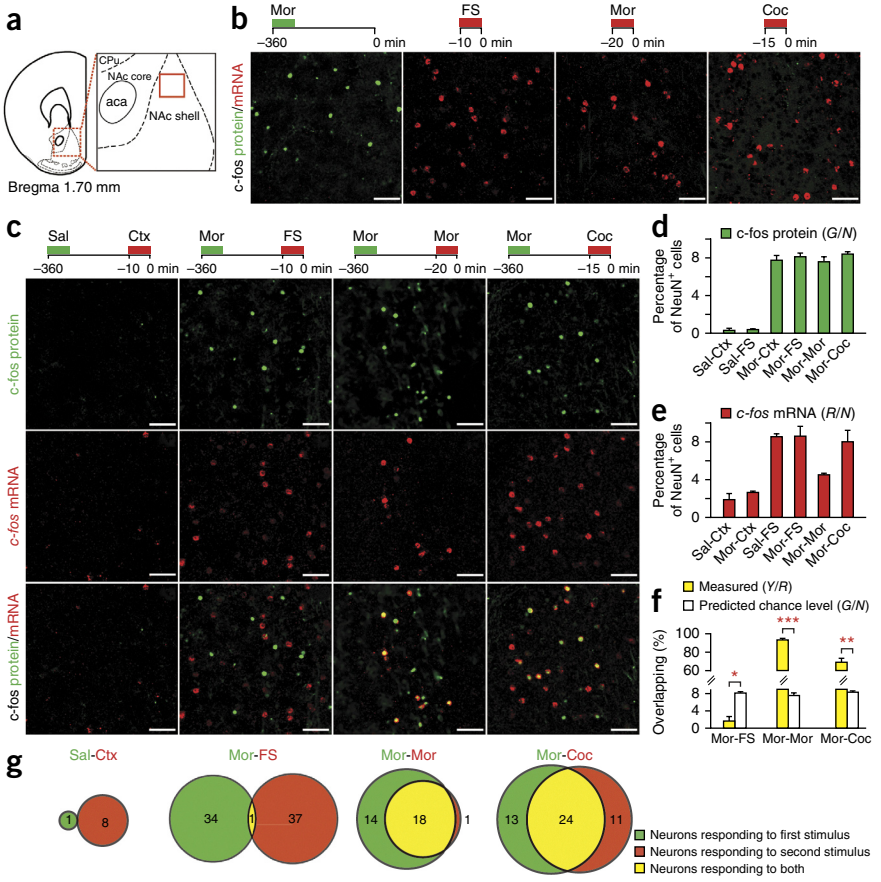

Figure 4 Intermingled neural representations of morphine and foot shock in NAc_{DMS}. (**a**) Schematic illustrating the location of NAc. The red dashed box indicates the field of the image taken with a 10× objective for quantification analysis. The red solid box indicates the position of the magnified images of the NAc_{DMS} shown in **c**. CPu, caudate putamen; aca, anterior commissural, anterior part. (**b**) Only c-fos protein signals (green) were present at 360 min post morphine and only *c-fos* mRNA signals (red) were present at 10 min post foot shock, 20 min post morphine and 15 min post cocaine. (**c**) Representative images showing the green (c-fos protein), red (*c-fos* mRNA) and merged channels of TAI-FISH double labeling from four experiments: saline-context, morphine–foot shock, morphine-morphine and morphine-cocaine. (**d**,**e**) Percentage of neurons expressing c-fos protein (**d**) and mRNA (**e**) in the rostral NAc_{DMS} in the six TAI-FISH experimental conditions: saline-context, saline–foot shock, morphine-context, morphine–foot shock, morphine-morphine and morphine-cocaine. Note that the second morphine injection activated fewer neurons in the morphine-morphine condition than the first morphine injection, potentially as a result of desensitization. (**f**) Percentage of overlap in the morphine–foot shock, morphine-morphine and morphine-cocaine double-labeling experiments in the rostral NAc_{DMS}. Measured overlaps were calculated as *Y*/*R*. Predicted chance level of overlaps was calculated as *G*/*N* (Online Methods). (**g**) Scaled Venn diagrams showing the number of green, red and yellow neurons in rostral NAc_{DMS} in the four experimental conditions shown in **c**. More than 400 neurons per mouse from three mice were counted for each group. Paired *t* test adjusted by Benjamini-Hochberg procedure controlling the false discovery rate. $*P < 0.05$, $**P < 0.01$, $***P < 0.001$. Scale bars represent 50 μm. Error bars represent s.e.m.

conditioning[26,27]. To investigate whether morphine-induced c-fos$^+$ neurons in CEl are of the CEl_{off} type, we examined the colocalization of c-fos and protein kinase C-δ (*PKC-δ*, *Prkcd*), a molecular marker of CEl_{off} neurons[27]. Notably, 95 ± 1% of morphine-induced c-fos$^+$ neurons expressed *PKC-δ*, as revealed by double labeling (**Fig. 2h–j**), suggesting that morphine mostly activated the OFF neurons in the CEl. Collectively, these results suggest that morphine and foot shock activate distinct sub-nuclei in CEA that have opposing roles in fear output.

In addition to CEA, several other forebrain regions also responded to only one of the stimuli. For example, the amygdalostriatal transition area (AStr) and MEA responded strongly to foot shock, but not to morphine (**Fig. 2b–d** and **Supplementary Fig. 4**). Conversely, the oval nucleus of BST, BSTov, responded to morphine, but not to foot shock (**Supplementary Fig. 5**).

Convergent pattern in PVN

The PVN is a hypothalamic nucleus known to be activated by a variety of stressful and physiological changes, and controls the hypothalamic-pituitary-adrenal (HPA) axis and glucocorticoid release[29] (**Fig. 3**). At 150 min post foot shock, the *c-fos* mRNA signal in the PVN was diminished, but the protein signal was still robust; at 20 min post morphine injection, the *c-fos* mRNA signal peaked, but the protein signal had not appeared (**Fig. 3b** and **Supplementary Figs. 1** and **3**). Thus, we chose to administer foot shock at 150 min and morphine at 20 min prior to killing the animals for the I-FISH analysis in the PVN.

In this foot shock–morphine configuration, foot shock and morphine each induced strong activation in the PVN, recruiting 58 ± 3% (the number of green neurons (*G*) divided by the number of NeuN$^+$ neurons (*N*)) and 63 ± 2% (*R*/*N*) of total neurons, respectively (**Fig. 3c–e**). For the control, saline injection in the home cage or exposure to the foot shock context induced little signal in the PVN (**Fig. 3c–e**). Notably, 79 ± 3% of the green cells were also red, indicating that 79% of foot shock–activated neurons also responded to morphine (**Fig. 3c**,**f**). This overlap ratio was close to the 78 ± 5% overlap ratio in the foot shock–foot shock configuration, in which two identical foot shock stimuli were applied sequentially (**Fig. 3c**,**f**). These findings suggest that nearly identical neural populations in the PVN were involved in the processing of both morphine and foot shock, in a valence-independent manner. In addition to the PVN, neurons activated by morphine and foot shock also displayed a partially convergent pattern in the fusiform nucleus of the BST (BSTfu; **Supplementary Fig. 6**).

Intermingled pattern in NAc and LSv

The NAc is an essential component of the brain's reward pathway, located in the ventral striatum (**Fig. 4a**). On the basis of NAc time course mapping (**Fig. 4b** and **Supplementary Figs. 1** and **3**), we injected morphine 360 min and delivered foot shock 10 min before killing the animals for TAI-FISH analysis in NAc.

The *c-fos* signals induced by morphine and foot shock were mostly located in the medial shell region of the NAc (**Fig. 4a**,**b**). In the dorsomedial shell of the NAc (NAc_{DMS}), morphine and foot shock each induced activation of similar numbers, 8.1 ± 0.4% (*G*/*N*) and 8.6 ± 1.0% (*R*/*N*), of total neurons, respectively (**Fig. 4c–e**). Notably, the green and red signals were distributed in a salt-and-pepper

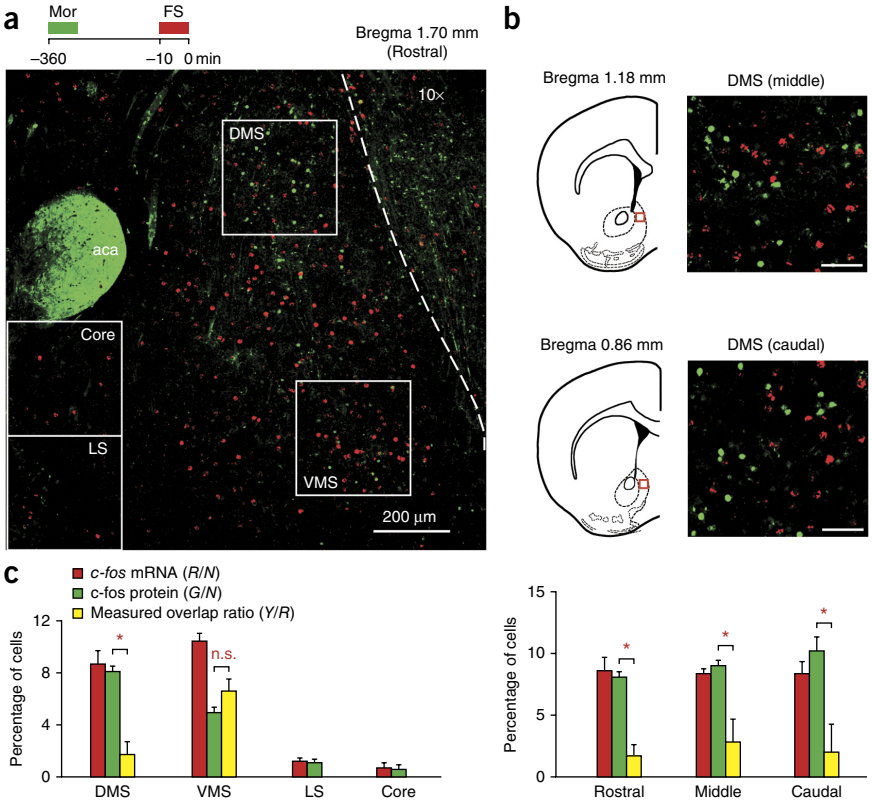

Figure 5 Neural representations of morphine and foot shock in the whole field of NAc revealed by TAI-FISH. (**a**) Representative image of TAI-FISH dual-labeling for morphine–foot shock in the whole field of rostral NAc. DMS, dorsomedial shell; VMS, ventromedial shell; LS, lateral shell. White dashed line indicates the boundary of the NAc. This image is one single microscopic field taken with a 10× objective, illustrating the potential of TAI-FISH to map large brain areas. (**b**) Representative images of TAI-FISH labeling for morphine–foot shock in the NAc_{DMS} at middle and caudal sections. Red boxes indicate position of the magnified images of the NAc_{DMS} shown on the right. Scale bars represent 50 µm. (**c**) Quantification of neurons expressing the c-fos protein (green), *c-fos* mRNA (red) or both (yellow) in different parts of the rostral NAc (left), or from the rostral to caudal NAc_{DMS} (right). Note that green bars (*G*/*N*) also represent the predicted chance level of overlap. More than 300 neurons per mouse from three mice were counted for each group. Paired *t* test adjusted by Benjamini-Hochberg procedure controlling the false discovery rate. $^*P < 0.05$; n.s., not significant, $P = 0.07$. Error bars represent s.e.m.

pattern with an overlap ratio of only 1.7 ± 1.0% (**Fig. 4c**), which was significantly lower than predicted chance level (8.1 ± 0.4%, $P = 0.017$; **Fig. 4f**; predicted chance level of overlap was calculated as *G*/*N*, Online Methods). In contrast, the overlaps in the morphine-morphine, and morphine-cocaine configuration reached 93 ± 2% and 68 ± 5%, respectively (**Fig. 4c–g**). The intermingled pattern remained the same from the rostral to the caudal side of the NAc_{DMS} (**Fig. 5a–c**). In the ventromedial shell (NAc_{VMS}), more neurons responded to foot shock and the overlap (6.6 ± 1.0%) was close to chance level (4.9 ± 0.5%, $P = 0.07$; **Fig. 5a–c**). These results suggest that, in the NAc_{DMS}, two distinct, intermingled populations of neurons encoded the response to morphine and foot shock. In addition to the NAc, neurons activated by morphine and foot shock were also intermingled in the posterior ventral part of the LS (LSv), an area that processes pleasant sensations and stress responses[30] (**Supplementary Fig. 7**).

NAc neurons are divided into two morphologically indistinguishable, but intermingled, subpopulations, D1- and D2-MSNs, which define the Go and NoGo pathways for action[22–24]. We asked whether the morphine-induced and foot shock–induced *c-fos*$^+$ neurons segregated with one of these two subgroups. Co-staining of c-fos FIHC with the D1 or D2 FISH revealed that the majority of morphine-induced c-fos$^+$ neurons expressed D1 (80 ± 0.8% D1$^+$ and 21 ± 2.1% D2$^+$; **Fig. 6a,b**), a percentage similar to that previously reported for cocaine-induced c-fos$^+$ neurons using *Drd1-GFP* and *Drd2-GFP* mice[31]. Among the foot shock–induced c-fos$^+$ neurons, D2$^+$ neurons predominated, but D1$^+$ neurons also contributed a substantial portion (62 ± 0.9% D2$^+$ and 39 ± 0.9% D1$^+$; **Fig. 6a,b**). Similar ratios were present from rostral to caudal NAc_{DMS} (**Fig. 6c**).

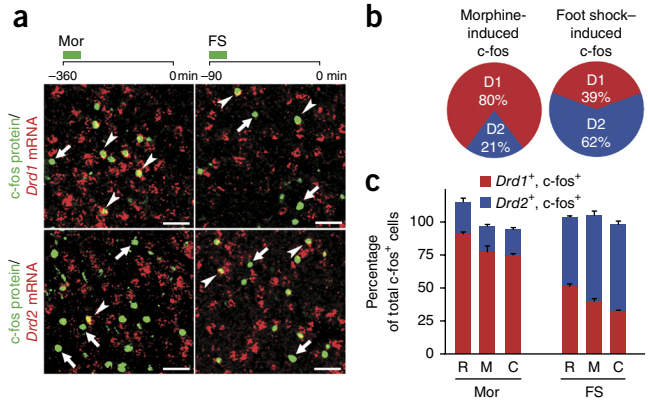

Figure 6 Heterogeneity in D1- and D2-MSNs in the NAc in response to morphine and foot shock. (**a**) Representative images showing colabeling of *Drd1* or *Drd2* mRNA with c-fos protein in the NAc_{DMS}, as induced by morphine or foot shock. Arrowheads indicate colocalized signals. Arrows indicate single c-fos protein signals. Scale bars represent 30 µm. (**b**) Percentage of morphine-induced c-fos$^+$ (left) and foot shock–induced c-fos$^+$ (right) neurons that expressed D1 (red) or D2 (blue). Counting was performed for the whole NAc_{DMS}. (**c**) Colabeling of *c-fos* signals with D1 and D2 markers along the rostral-caudal axis in the NAc_{DMS}. R, rostral; M, middle; C, caudal. Error bars represent s.e.m.

Representations of multiple emotional cues in NAc

Does the intermingled pattern of activation in the NAc_{DMS} reflect the representation of emotional values or other features (for example, specific sensory properties) associated with morphine or foot shock? To distinguish between these possibilities, we further tested dual labeling with an additional appetitive stimulus, chocolate, and an additional aversive stimulus, restraint, which are experienced through markedly different sensory modalities, and determined their optimal application time for dual labeling (**Fig. 7a** and **Supplementary Fig. 3c**). First, when pairing morphine with the natural reward, chocolate (morphine-chocolate), mice were injected with morphine and then fed chocolate 15 min before being killed. The chocolate-induced *c-fos* mRNA signals

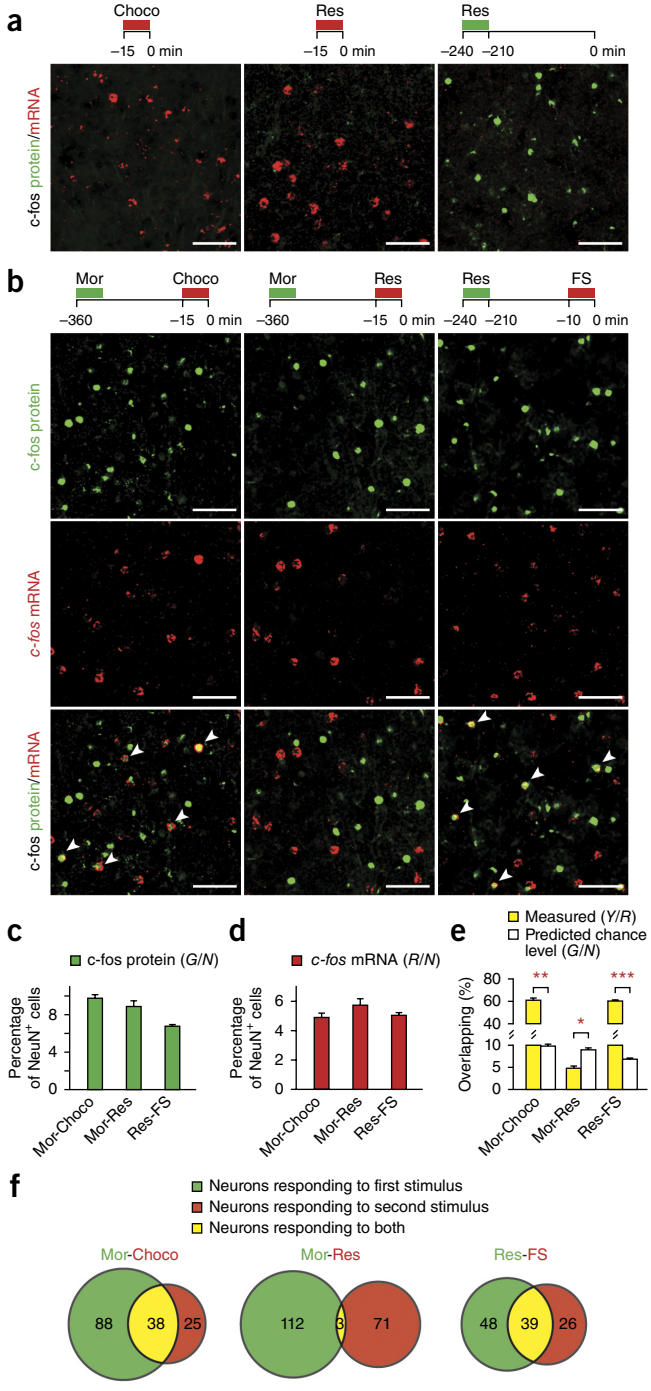

Figure 7 Representations of multiple positive and negative emotional cues in NAc. (**a**) Only *c-fos* mRNA signals (red) were present at 15 min post chocolate (Choco) and 15 min post restraint (Res), and only *c-fos* protein signals (green) were present at 240 min after the start of restraint in NAc_{DMS}. (**b**) Representative images showing green (c-fos protein), red (*c-fos* mRNA) and merged channels of TAI-FISH double labeling in the NAc_{DMS} following sequential stimulation of morphine-chocolate, morphine-restraint and restraint–foot shock. White arrowheads indicate merged signals. (**c**–**e**) Percentage of neurons expressing c-fos protein (**c**) and mRNA (**d**), and percentage of overlap (**e**) in the NAc_{DMS} in the morphine-chocolate, morphine-restraint and restraint–foot shock TAI-FISH experiment. (**f**) Scaled Venn diagrams showing the number of green, red and yellow neurons in the whole NAc_{DMS} in the four experimental conditions shown in **c**. Counting was performed for the whole NAc_{DMS}. More than 400 neurons per mouse from 3 mice were counted for each group. Paired *t* test adjusted by Benjamini-Hochberg procedure controlling the false discovery rate. $^{*}P < 0.05$, $^{**}P < 0.01$, $^{***}P < 0.001$. Scale bars represent 50 μm. Error bars represent s.e.m.

were generally weaker and fewer than those induced by morphine (**Fig. 7b**). However, there was a great degree of overlap (61 ± 2.6%) between the chocolate- and morphine-activated cell groups in NAc_{DMS} (**Figs. 7b–f** and **8**). In contrast, when pairing morphine with another aversive stimulus, restraint (morphine-restraint), the overlap was only 4.6 ± 0.8% (**Figs. 7b**,**e**,**f** and **8**). Finally, in the configuration in which two aversive stimuli were sequentially applied (restraint–foot shock), the overlap ratio reached 60 ± 1.5% (**Figs. 7b–f** and **8**). These results revealed that emotional stimuli of the same valence activated largely overlapping neural ensembles in the NAc, whereas stimuli of different valence activated distinct neural populations (**Fig. 8**).

DISCUSSION

We applied TAI-FISH to simultaneously visualize the neural substrates of morphine and foot shock in the same mouse brain. We found that the neural representation of these emotional stimuli were stable and stereotypic. In all the brain structures examined, sequential applications of the same emotional stimulus always activated highly overlapping neural groups (**Figs. 2e**,**g**, **3c**,**f** and **4c**,**f**), suggesting that the brain uses dedicated neural ensembles to encode emotional stimuli. The same principle has been demonstrated for the hippocampal encoding of spatial information[32].

We also found that the two emotional stimuli evoked largely distinct neural ensembles throughout the limbic forebrain despite activating many of the same regions (**Fig. 8a** and **Supplementary Fig. 8**). This anatomical map includes distinct patterns of interaction, segregated (for example, in CEA), convergent (for example, in the PVN) and intermingled (for example, in the NAc and posterior LSv), between the two neural ensembles. Notably, in the NAc_{DMS}, neurons responding to two stimuli of different valence (morphine versus foot shock) were almost equal in number (~8% of the neurons in the NAc_{DMS}), but were spatially intermingled (**Fig. 4**). In contrast, there was a large overlap between neural ensembles representing the same valence, morphine versus chocolate or foot shock versus restraint, in the NAc_{DMS} (**Figs. 7** and **8b**). These observations revealed the existence of a functional valence map in the NAc.

An extensive amount of work has focused on the function of NAc in appetitive motivation and positive reinforcement, as well as in aversive motivation[28,33–39]. How does the NAc differentially encode rewarding and aversive stimuli? Considering that D1-MSNs define the Go pathway that facilitates action, and D2-MSNs define the NoGo pathway that suppresses action[22–24], an appealing model is that the D1- and D2-MSNs in the NAc differentially code appetitive and aversive information[40,41]. We found that D1- and D2-MSNs could respond to both morphine and foot shock stimuli, but with different preference: the number of D1-MSNs responding to morphine was roughly twice that of those responding to foot shock (80% versus 39%, as the total number of morphine- and foot shock–induced were similar), whereas the number of D2-MSNs responding to foot shock was threefold greater than those responding to morphine (62% versus 21%) in NAc_{DMS} (**Fig. 6b**). This asymmetrical distribution would enable positive and negative emotional stimuli to differentially activate the Go and NoGo action pathways, respectively, and direct opposite behavioral outputs. However, we found that D1-MSNs overall contributed to a substantial portion (about 40%) of c-fos^{+} neurons activated by the aversive foot shock stimulus. This fraction was much

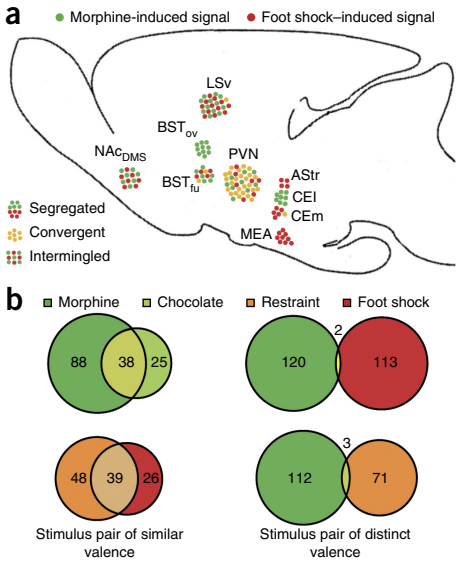

Figure 8 An emotional valence map in the forebrain. (**a**) Summary of patterns of interaction between neural representations of morphine and foot shock in different regions of the limbic forebrain, as revealed by TAI-FISH (one dot represents $n = 5$ neurons counted from representative sections in each corresponding region). (**b**) Scaled Venn diagram summarizing the interaction of multiple positive and negative emotion representations in the NAc_{DMS}. The numbers of c-fos$^+$ neurons counted from the whole NAc_{DMS} (sampled from a 300 μm × 300 μm area of each rostro-caudal level, $n = 3$ mice) are labeled in the circle. Stimuli of similar emotional valences had much larger overlap than those of opposite valences.

greater than, and could not be accounted for by, the 10–17% of MSNs coexpressing D1 and D2 receptors[31,42]. Thus, the map identified here suggests additional complexity in the functional organization of the NAc and raises the interesting question on the function of the foot shock–activated D1-MSNs.

What is the functional relevance underlying the intermingled pattern of valence coding in the NAc_{DMS}? This mosaic organization is reminiscent of the early-stage functional map of several sensory representations, including the distribution of on and off cells in the retina[43], where lateral inhibition is an important feature of the neural network architecture, serving to enhance contrast. Indeed, the axon collaterals of MSNs in the NAc can inhibit neighboring MSNs through GABAergic synapses[44], providing an anatomical basis for the lateral inhibition. It is therefore interesting to speculate that the intermingled pattern of valence representation in the NAc may allow neurons of opposite emotional values to inhibit each other and compete, directing action outputs in a more discrete fashion.

Choice of emotional stimuli

We chose to use unconditioned stimuli (US, stimuli that can naturally trigger emotional responses) instead of conditioned stimuli (CS, previously neutral stimuli that become capable of evoking emotional responses after association with US) in our procedure for several reasons. First, US generally elicit a stronger response than CS. Second, no training is required for the protocol. Third, giving CS without the actual US could trigger a reward-error signal[45]. Finally, US-induced signals are independent of previous learning, thereby eliminating the effects of adaptation and memory. This may explain why *c-fos* signals activated by foot shock (in the CEm; **Fig. 2**) distributed differently from those activated by recall of fear memory (a type of CS; in the CEl[46]).

However, there are potential compounding effects associated with US that should be cautioned. For example, morphine, as a drug, may elicit complex effects in addition to an appetitive sensation. At a very low dosage (0.05 mg per kg), morphine can be aversive[25,47]. Morphine may also have a lasting effect on emotion. To address these concerns, we first carried out a conditioned place preference test to confirm that morphine was appetitive at the dosage injected (15 mg per kg; **Fig. 1d**). Next, to confirm that morphine's potential lingering effect did not alter the negative valence associated with foot shock, we tested real-time place preference for foot shock at 6 h after morphine injection. Foot shock still induced strong place aversion in the morphine-injected group, similar to the saline-injected group (**Supplementary Fig. 9**), suggesting that earlier morphine did not invert or reduce the sensation of foot shock as a negative stimulus. Furthermore, foot shock–induced *c-fos* signals were indistinguishable if mice were treated with saline or with morphine earlier (**Fig. 4d**).

Strengths and limitations of TAI-FISH

Behavioral neuroscience has long called for a molecular imaging technique that can compare activity patterns of different physiological states at the cellular level across the whole brain[7]. Several innovative IEG-based functional imaging methods have been developed to examine the neural correlates of two distinct stimuli: I-FISH[17], cellular compartment analysis of temporal activity by FISH (catFISH, employing the distinct time course of nuclear versus cytoplasmic localization of IEG mRNA[32,48]), and TetTag[49] and TRAP mice[50], which use genetic mouse models. CatFISH requires high-magnification (for example, 64×) imaging to differentiate the subcellular localization. In contrast, I-FISH can be performed with low magnification (for example, 10×), making it easier to map large brain areas or even the whole brain[21] (**Fig. 5a**). However, the strict separation of the IEG protein and mRNA time courses is not always satisfied in different brain regions or for different stimuli (for example, in the NAc when morphine was applied as the first stimulus; **Fig. 1c**), which may have impeded the general application of I-FISH. TAI-FISH improves I-FISH by introducing a tyramide-amplification step for FIHC. This step extended the time course of the protein signal (**Fig. 1c**), enabling better separation of the mRNA and protein time courses and greatly improving the capacity of the method. Indeed, examination of half of the brain structures in this study (NAc, LSv and BST) would not have been possible without the FIHC tyramide amplification. Moreover, the time interval between the two stimuli for TAI-FISH (several hours) is substantially longer than that for catFISH (~30 min), which could be a useful feature when the interference between the two behaviors or stimuli needs to be minimized.

TAI-FISH does have limitations that are intrinsic to IEG imaging approaches. First, it is unable to detect neurons below the detection threshold or inhibited by a stimulus, resulting in a partial map. Second, not all neurons can express all IEGs abundantly. For example, unlike reports using the IEG *Arc* as a probe, we detected little *c-fos* signals in the hippocampus by morphine or foot shock. Third, activity under control conditions can be high in some brain areas. For example, the medial prefrontal cortex and anterior LS showed substantial *c-fos* signals by saline injection and context alone, and were therefore not included in the analysis. Finally, the mRNA signal of the first stimulus can be long-lasting (for example, in the basal lateral amygdala and dorsal raphe, presumably as a result of recurrent activation; **Supplementary Fig. 2**) or the protein signal of the first stimulus can decay too fast, precluding the separation of the mRNA and protein time courses. Nevertheless, it is hopeful that some of these problems can be overcome by using different IEG genes, such as *Arc*, *zif268* or *Homer1a*, which have different induction time courses and expression profiles. In addition, TAI-FISH can be used in conjunction with

catFISH to give a more complete map, or even triple-epoch map when needed. In the VTA region, there was strong background fluorescent staining of the axon fibers. It would be worth trying non–fluorescence-based chemical staining methods (for example, NBT/BCIP for mRNA and DAB for protein) to re-examine this area.

In conclusion, TAI-FISH permits global whole-brain dual-activity mapping in wild-type mice with single-cell resolution. It provides a powerful methodology, complementing electrophysiological and other functional imaging methods, for identifying neural networks responsible for the internal representations of different behavioral and emotional states. The valence map that we identified may allow the exciting possibility of specifically manipulating the appetitive and aversive behaviors.

METHODS

Methods and any associated references are available in the online version of the paper.

Note: Any Supplementary Information and Source Data files are available in the online version of the paper.

ACKNOWLEDGMENTS

We thank J. Feldman for critical review of the manuscript, S. Sarah, H. Kessels, A. Roe and M. Poo for comments on the manuscript, and S. Song, J. Huang, B. Lu and members of the Hu laboratory for stimulating discussions. This work was supported by the Chinese 973 Program (2011CBA00400), the Strategic Priority Research Program (B) of the Chinese Academy of Sciences (XDB02030004), the One Hundred Talents Program and the Outstanding Youth Grant (to H.H.).

AUTHOR CONTRIBUTIONS

J.X. designed the study and performed the TAI-FISH experiments. Q.Z. and Tao Zhou contributed to the TAI-FISH experiments. Ting-ting Zhou tested the time course for chocolate stimulation. Y.C. performed the statistical analysis. H.H. conceived the idea, designed the study and wrote the manuscript with input from J.X., Q.Z. and Tao Zhou.

COMPETING FINANCIAL INTERESTS

The authors declare no competing financial interests.

1. LeDoux, J.E. *The Emotional Brain: the Mysterious Underpinnings of Emotional Life* (Simon & Schuster, New York, 1996).
2. Panksepp, J. Affective neuroscience: the foundations of human and animal emotions. (Oxford University Press, New York, 1998).
3. Lang, P.J. & Davis, M. Emotion, motivation, and the brain: reflex foundations in animal and human research. *Prog. Brain Res.* **156**, 3–29 (2006).
4. Chen, X., Gabitto, M., Peng, Y., Ryba, N.J. & Zuker, C.S. A gustotopic map of taste qualities in the mammalian brain. *Science* **333**, 1262–1266 (2011).
5. Marshall, W.H., Woolsey, C.N. & Bard, P. Observations on cortical somatic sensory mechanisms of cat and monkey. *J. Neurophysiol.* **4**, 1–24 (1941).
6. Mombaerts, P. *et al.* Visualizing an olfactory sensory map. *Cell* **87**, 675–686 (1996).
7. LeDoux, J. Rethinking the emotional brain. *Neuron* **73**, 653–676 (2012).
8. Anderson, D.J. & Adolphs, R. A framework for studying emotions across species. *Cell* **157**, 187–200 (2014).
9. Johnson, Z.V., Revis, A.A., Burdick, M.A. & Rhodes, J.S. A similar pattern of neuronal Fos activation in 10 brain regions following exposure to reward- or aversion-associated contextual cues in mice. *Physiol. Behav.* **99**, 412–418 (2010).
10. Freed, P.J., Yanagihara, T.K., Hirsch, J. & Mann, J.J. Neural mechanisms of grief regulation. *Biol. Psychiatry* **66**, 33–40 (2009).
11. Lammel, S. *et al.* Input-specific control of reward and aversion in the ventral tegmental area. *Nature* **491**, 212–217 (2012).
12. Matsumoto, M. & Hikosaka, O. Two types of dopamine neuron distinctly convey positive and negative motivational signals. *Nature* **459**, 837–841 (2009).
13. Morrison, S.E. & Salzman, C.D. The convergence of information about rewarding and aversive stimuli in single neurons. *J. Neurosci.* **29**, 11471–11483 (2009).
14. Roitman, M.F., Wheeler, R.A. & Carelli, R.M. Nucleus accumbens neurons are innately tuned for rewarding and aversive taste stimuli, encode their predictors, and are linked to motor output. *Neuron* **45**, 587–597 (2005).
15. Shabel, S.J. & Janak, P.H. Substantial similarity in amygdala neuronal activity during conditioned appetitive and aversive emotional arousal. *Proc. Natl. Acad. Sci. USA* **106**, 15031–15036 (2009).
16. Taha, S.A. & Fields, H.L. Encoding of palatability and appetitive behaviors by distinct neuronal populations in the nucleus accumbens. *J. Neurosci.* **25**, 1193–1202 (2005).
17. Chaudhuri, A., Nissanov, J., Larocque, S. & Rioux, L. Dual activity maps in primate visual cortex produced by different temporal patterns of zif268 mRNA and protein expression. *Proc. Natl. Acad. Sci. USA* **94**, 2671–2675 (1997).
18. Chan, R.K.W., Brown, E.R., Ericsson, A., Kovacs, K.J. & Sawchenko, P.E. A comparison of 2 immediate-early genes, c-Fos and Ngfi-B, as markers for functional activation in stress-related neuroendocrine circuitry. *J. Neurosci.* **13**, 5126–5138 (1993).
19. Greenberg, M.E. & Ziff, E.B. Stimulation of 3T3 cells induces transcription of the c-fos proto-oncogene. *Nature* **311**, 433–438 (1984).
20. Morgan, J.I., Cohen, D.R., Hempstead, J.L. & Curran, T. Mapping patterns of c-fos expression in the central nervous system after seizure. *Science* **237**, 192–197 (1987).
21. Farivar, R., Zangenehpour, S. & Chaudhuri, A. Cellular-resolution activity mapping of the brain using immediate-early gene expression. *Front. Biosci.* **9**, 104–109 (2004).
22. Gerfen, C.R. The neostriatal mosaic: multiple levels of compartmental organization in the basal ganglia. *Annu. Rev. Neurosci.* **15**, 285–320 (1992).
23. Kreitzer, A.C. Physiology and pharmacology of striatal neurons. *Annu. Rev. Neurosci.* **32**, 127–147 (2009).
24. Surmeier, D.J., Ding, J., Day, M., Wang, Z. & Shen, W. D1 and D2 dopamine-receptor modulation of striatal glutamatergic signaling in striatal medium spiny neurons. *Trends Neurosci.* **30**, 228–235 (2007).
25. Bechara, A. & van der Kooy, D. Opposite motivational effects of endogenous opioids in brain and periphery. *Nature* **314**, 533–534 (1985).
26. Ciocchi, S. *et al.* Encoding of conditioned fear in central amygdala inhibitory circuits. *Nature* **468**, 277–282 (2010).
27. Haubensak, W. *et al.* Genetic dissection of an amygdala microcircuit that gates conditioned fear. *Nature* **468**, 270–276 (2010).
28. Koob, G.F. & Volkow, N.D. Neurocircuitry of addiction. *Neuropsychopharmacology* **35**, 217–238 (2010).
29. Sawchenko, P.E., Li, H.Y. & Ericsson, A. Circuits and mechanisms governing hypothalamic responses to stress: a tale of two paradigms. *Prog. Brain Res.* **122**, 61–78 (2000).
30. Sheehan, T.P., Chambers, R.A. & Russell, D.S. Regulation of affect by the lateral septum: implications for neuropsychiatry. *Brain Res. Brain Res. Rev.* **46**, 71–117 (2004).
31. Bertran-Gonzalez, J. *et al.* Opposing patterns of signaling activation in dopamine D1 and D2 receptor–expressing striatal neurons in response to cocaine and haloperidol. *J. Neurosci.* **28**, 5671–5685 (2008).
32. Guzowski, J.F., McNaughton, B.L., Barnes, C.A. & Worley, P.F. Environment-specific expression of the immediate-early gene Arc in hippocampal neuronal ensembles. *Nat. Neurosci.* **2**, 1120–1124 (1999).
33. Dölen, G., Darvishzadeh, A., Huang, K.W. & Malenka, R.C. Social reward requires coordinated activity of nucleus accumbens oxytocin and serotonin. *Nature* **501**, 179–184 (2013).
34. Kreitzer, A.C. & Malenka, R.C. Striatal plasticity and basal ganglia circuit function. *Neuron* **60**, 543–554 (2008).
35. Russo, S.J. *et al.* The addicted synapse: mechanisms of synaptic and structural plasticity in nucleus accumbens. *Trends Neurosci.* **33**, 267–276 (2010).
36. Salamone, J.D. The involvement of nucleus accumbens dopamine in appetitive and aversive motivation. *Behav. Brain Res.* **61**, 117–133 (1994).
37. Sesack, S.R. & Grace, A.A. Cortico-basal ganglia reward network: microcircuitry. *Neuropsychopharmacology* **35**, 27–47 (2010).
38. Wheeler, R.A. & Carelli, R.M. Dissecting motivational circuitry to understand substance abuse. *Neuropharmacology* **56**, 149–159 (2009).
39. Reynolds, S.M. & Berridge, K.C. Positive and negative motivation in nucleus accumbens shell: bivalent rostrocaudal gradients for GABA-elicited eating, taste "liking"/"disliking" reactions, place preference/avoidance, and fear. *J. Neurosci.* **22**, 7308–7320 (2002).
40. Hikida, T., Kimura, K., Wada, N., Funabiki, K. & Nakanishi, S. Distinct roles of synaptic transmission in direct and indirect striatal pathways to reward and aversive behavior. *Neuron* **66**, 896–907 (2010).
41. Kravitz, A.V., Tye, L.D. & Kreitzer, A.C. Distinct roles for direct and indirect pathway striatal neurons in reinforcement. *Nat. Neurosci.* **15**, 816–818 (2012).
42. Lee, K.W. *et al.* Cocaine-induced dendritic spine formation in D1 and D2 dopamine receptor–containing medium spiny neurons in nucleus accumbens. *Proc. Natl. Acad. Sci. USA* **103**, 3399–3404 (2006).
43. Kuffler, S.W. Discharge patterns and functional organization of mammalian retina. *J. Neurophysiol.* **16**, 37–68 (1953).
44. Taverna, S., Ilijic, E. & Surmeier, D.J. Recurrent collateral connections of striatal medium spiny neurons are disrupted in models of Parkinson's disease. *J. Neurosci.* **28**, 5504–5512 (2008).
45. Schultz, W., Dayan, P. & Montague, P.R. A neural substrate of prediction and reward. *Science* **275**, 1593–1599 (1997).
46. Scicli, A.P., Petrovich, G.D., Swanson, L.W. & Thompson, R.F. Contextual fear conditioning is associated with lateralized expression of the immediate early gene c-fos in the central and basolateral amygdalar nuclei. *Behav. Neurosci.* **118**, 5–14 (2004).
47. Switzman, L., Hunt, T. & Amit, Z. Heroin and morphine: aversive and analgesic effects in rats. *Pharmacol. Biochem. Behav.* **15**, 755–759 (1981).
48. Lin, D. *et al.* Functional identification of an aggression locus in the mouse hypothalamus. *Nature* **470**, 221–226 (2011).
49. Reijmers, L.G., Perkins, B.L., Matsuo, N. & Mayford, M. Localization of a stable neural correlate of associative memory. *Science* **317**, 1230–1233 (2007).
50. Guenthner, C.J., Miyamichi, K., Yang, H.H., Heller, H.C. & Luo, L. Permanent genetic access to transiently active neurons via TRAP: targeted recombination in active populations. *Neuron* **78**, 773–784 (2013).

ONLINE METHODS

Animals. All animal studies were approved by the institutional Animal Care and Use Committee of the Institute of Neuroscience, Chinese Academy of Sciences. 3-month-old male C57BL/6 mice were used for this study and housed four per cage in a room with a 12-h light/dark cycle (7:00 a.m. to 7:00 p.m.), in stable conditions of temperature (22 °C) and humidity (60%), with food and water *ad libitum*. Behavioral studies were conducted between 1:00 and 5:00 p.m. For morphological studies, mice were divided into two per cage 4 d before the start of the experiment to ensure they received the same treatment, were killed within 10 s of the treatment termination and were perfused by two people simultaneously within ~10 min (to reduce cross-influence on cagemates). All mice were killed between 3:30 and 5:30 p.m. after each treatment. With these precautions taken, we found that basal levels of *c-fos* expression in unstimulated mice were uniformly low throughout the limbic forebrain, except in the paraventricular thalamus and suprachiasmatic nucleus, despite some background staining in various cortical regions (mostly in the piriform cortex, and some weak signals in the visual and motor cortices).

Drugs and treatments. Morphine-HCl (15 mg per kg, i.p., Shenyang Pharmaceutical) and cocaine-HCl (20 mg per kg, i.p., Shenyang Pharmaceutical) were dissolved in 0.9% NaCl (wt/vol, saline). 6 g of crumbled milk chocolate (Dove), similar in size to rice grains, were scattered in the home cage 15 min before mice were sacrificed. All mice began eating the chocolate within 3–5 min. For aversive treatments, 15 randomly arranged foot shocks (1 mA, 2 s) were administered on mice within 10 min in a fear conditioning chamber (Coulbourn Instruments). Restraint stress was performed in the home cage by placing mice in a short 9-cm-long transparent Plexiglas tube (3.2-cm inside diameter), which lasted for 30 (as first stimulus) or 15 min (as second stimulus).

Tissue preparation. Mice were rapidly anesthetized with chloral hydrate (10%, wt/vol, i.p.) and sequentially perfused transcardially with ice-cold 0.01 M phosphate-buffered saline (PBS, pH 7.4) and paraformaldehyde (4% in PBS, wt/vol, Sigma). Brains were postfixed for 48 h in the same fixative solution and stored at 4 °C. After cryoprotection with 30% sucrose (wt/vol) in PBS, three serials of 40-μm-thick coronal sections were cut on a cryostat (CM1950, Leica) and immediately subjected to histochemical staining.

FISH and FIHC. Brain slices were sequentially subjected to FISH and FIHC staining. For FISH, all solutions used for the hybridization were prepared using RNase-free reagents and diethylpyrocarbonate (DEPC)-treated double deionized water (ddH_2O). Throughout the hybridization process, all instruments were RNase-decontaminated using RNase ZAP solution (Ambion). Probes against *c-fos*, *PKC-δ*, *Drd1a* and *Drd2* were constructed according to the description on Allen Brain Atlas website (http://www.brain-map.org). All probes were cloned into pGEM-T vector (Promega). The RNA probes labeled by digoxygenin-UTP (Roche) were generated by *in vitro* transcription and dissolved at 1 μg ml^{-1} in the hybridization solution (50% formamide (vol/ vol), 5× SSC, 0.3 mg ml^{-1} yeast tRNA, 100 μg ml^{-1} heparin, 1× Denhardt's solution, 0.1% Tween 20 (vol/vol), 0.1% 3-[(3-cholamidopropyl) dimethylammonio]-1-propanesulfonate (CHAPS, wt/vol) and 5 mM EDTA). For FISH, free-floating sections were washed with 0.01 M PBS for 10 min and treated with 2% H_2O_2 (vol/vol) in 0.01 M PBS for 10 min, followed by another round of wash with PBS for 10 min at 25~28 °C. They were then treated with 0.3% Triton X-100 (vol/vol) in 0.01 M PBS for 20 min and acetylated by 0.25% acetic anhydride (vol/vol) in 0.1 M triethanolamine (pH 8.0) for 10 min, followed by two rounds of washing with PBS. Afterward, the sections were placed in the hybridization solution without probes for 1 h and incubated in the hybridization solution with the corresponding probes for 16–18 h at 60 °C. After hybridization, the sections were rinsed once and washed twice in 2× SSC for 15 min at 60 °C, followed by treatment with 2 μg ml^{-1} RNase A in 2× SSC at 37 °C for 30 min. They were further rinsed once and washed twice in 0.2× SSC for 30 min at 60 °C, followed by three rounds of wash in 0.01 M PBS containing 0.05% Tween 20 (PBT) for 10 min at 25~28 °C. The sections were blocked with 10% normal sheep serum (vol/vol) in PBT for 1 h at 25~28 °C and incubated in the same solution with sheep antibody to digoxygenin antibody (1:500, Roche 11207733910) at 4 °C overnight. On the second day, the sections were washed three times in PBT for 10 min and incubated in the amplification solution with cyanine 3 tyramide (1:100, PerkinElmer NEL744B001KT) for 20 min at 25~28 °C, followed by three rounds of washing in 0.01 M PBS for 10 min.

For FIHC, the sections were further incubated with rabbit antibody to c-fos (1:5,000 or 1:10,000; Calbiochem PC38) for 2 h at 25~28 °C and for 46 h at 4 °C. In the case of short treatment interval (≤3 h, in CEA, PVH and MEA regions), we visualized the protein signal directly via the Alexa Fluor 488 after binding of the goat antibody to rabbit (1:1,000, Invitrogen A11034) to the primary antibody. For the long treatment interval (≥4 h, in NAc, LSv and BST regions), an additional tyramide amplification step was introduced for all the experimental and control groups: the sections were further incubated with biotinylated rabbit antibody to goat antibody (1:400, Vector Labs BA5000) overnight at 4 °C, followed by reacting with horseradish peroxidase–conjugated streptavidin (1:800; Millipore 18-152) for 1.5 h at 25~28 °C. To inactivate the peroxidase used in the FISH, the sections were treated with 2% sodium azide (wt/vol) in 0.01 M PBS for 15 min at 25~28 °C immediately after the end of the primary antibody incubation. Finally, the protein signal was amplified and visualized using the same method as the FISH, but incubated with coumarin tyramide (1:150, PerkinElmer NEL703001KT). After three rounds of washing in 0.01 M PBS, the sections were mounted and stored at 4 °C until further analysis.

For calculation of the percentage of *c-fos*$^+$ cells, NeuN staining was performed on one serial of sections of the same animal. The sections were incubated with the mouse antibody to NeuN (1:1,000, Millipore MAB377) overnight at 4 °C and further reacted with Alexa Fluor 594 goat antibody to mouse (1:1,000, Invitrogen A31624).

Microscopy and image analysis. Fluorescent images were acquired using an Olympus Fluoview FV1000 confocal microscope with a 10× objective lens (NA = 0.40) under the control of the Olympus Fluoview FV1000 version 2.1b software. The thickness of sections covered in each image and used for quantification was 8.9 μm. The c-fos protein signal showed nuclear staining pattern, whereas its mRNA appeared mostly in the cytoplasm. Images shown in the figures were from the same region illustrated in the schematics according to specific neuroanatomical markers. Cell quantification was performed in a 300 × 300 μm square area for the NAc_{DMS}, NAc_{VMS}, NAc_{Core} and NAc_{LS} regions in **Figure 5a**, and in outlined areas for other brain regions. Signals were counted from one slice per mouse at the labeled Bregma position as outlined in the schematics of each corresponding figure. The control and experimental groups were processed in parallel. Images were coded and counting was performed in a blind fashion. Brightness and contrast adjustments were applied to the whole image. Positive protein signals should be solid round- or oval-shaped and have a diameter of 6~10 μm. Positive mRNA signals were typically particle clusters 6~10 μm in diameter. The background signal was determined by the mean gray value of an unlabeled brain region within the microscopic field. Intensity of mRNA and protein signals was at least 80-fold greater than that of the background value.

Calculation of overlap ratio. For calculation of the overlap ratio in the brain regions of convergent and intermingled patterns, we counted numbers of red (*R*), green (*G*) and yellow (*Y*) neurons from the double-labeled slices and the number of the NeuN-positive neurons (*N*) in a separate set of slices at the same location in designated regions. Note that *R* included both red and yellow neurons and *G* included both green and yellow neurons. We use *Y/R* to represent the measured overlap ratio. Since the chance for a given neuron to be both red and green (therefore appearing yellow) is *R/N* * *G/N*, the *predicted* $Y = R/N * G/N * N = R * G/N$. Therefore the predicted chance level of overlap ratio = predicted $Y/R = R * G/N/R = G/N$.

Behavioral procedures. Morphine conditioned place preference was performed in a three-chamber device (Med Associates). Briefly, it consisted of three phases. (i) Preconditioning. Mice were placed into the central compartment and allowed to freely explore the three compartments for 15 min on days 1 and 2. Between the left and right compartments, the less preferred one on day 2 was picked for morphine pairing on the conditioning day. The time spent in this compartment was used as the baseline. (ii) Conditioning. On day 3, mice were injected with morphine (15 mg per kg; i.p.) or saline and placed in the corresponding compartment for 30 min. (iii) Post-conditioning. On day 4, mice were handled in the same way as on day 1 and received no drug or saline administrations. Time spent in the compartment where mice received the morphine injection was used

doi:10.1038/nn.3813

as the post-conditioning time. Reference scores were expressed as the difference between the post-conditioning time and baseline.

The passive avoidance test was performed in a two-chamber device (Med Associates). One compartment was made of clear plastic and brightly illuminated while the other was covered and black. The grid-floor on both sides could be used to deliver foot shocks. On day 1, the mouse was placed in the lit compartment with the door open. After the mouse entered the dark side, the door was closed and 15 randomly arranged foot shocks (1 mA, 2 s), the same treatment as used in the morphological studies, were administered on mice within 10 min. 24 h later, mice were placed in the same lit compartment for 5 min with the door open. The latency to enter the dark side was automatically recorded by the device. The control group was treated with the same procedure but without foot shock delivery.

The real time place preference test was performed in a two-chamber device (Med Associates). The grid-floor on the left side was used to deliver foot shock. The mouse was i.p. injected with 15 mg per kg morphine or saline. 6 h after injection, the mouse was placed in the nonstimulus compartment. After the mouse entered the stimulus side, 1-mA foot shock was administered until the mouse moved into the nonstimulus compartment. The behavioral data was recorded by a CCD camera and analyzed by Ethovision software (Noldus) The number of attempts to enter the stimulus side was counted.

Statistical analysis. Statistical values were expressed as mean ± s.e.m., and error bars represent s.e.m. For behavioral experiments, Mann-Whitney *U* tests were conducted to compare group difference. For anatomical results, more than 250 neurons per mouse were counted from at least three mice. Paired *t* test was used when comparing measured and predicted ratios within same animals. For multiple comparisons, *P* values were adjusted using Benjamini-Hochberg procedure to control the false discovery rate. (Adjusted) *P* values less than 0.05 were considered statistically significant. Each representative image was successfully repeated at least three times.

A **Supplementary Methods Checklist** is available.